Vol 14 No 11, November 2005
1009-1963/2005/14(11)/2276-11
Chinese Physics
© 2005 Chin. Phys. Soc.
and IOP Publishing Ltd

Relationship between width of pulses and Lorentz factor expected from the light curve of fireball sources*

Zhang Fu-Wen(张富文)[a)b)c)†] and Qin Yi-Ping(覃一平)[a)b)]

[a)] *National Astronomical Observatories/Yunnan Observatory, Chinese Academy of Sciences, Kunming* 650011, *China*
[b)] *Physics Department, Guangxi University, Nanning* 530004, *China*
[c)] *Graduate School of The Chinese Academy of Sciences, Beijing* 100049, *China*

(Received 23 September 2004; revised manuscript received 31 January 2005)

Time profiles of many gamma-ray bursts consist of distinct pulses, which provides a possibility of characterizing the temporal structure of these bursts. We employ a simple model of highly symmetric fireballs to analyse the effect of the expansion speed on the light curve arising from different forms of local pulses. The relationship between the ratio r of the FWHM width of the rising phase of the light curve to that of the decaying phase and the Lorentz factor is investigated. The analysis shows that, when the rest frame radiation form is ignored, temporal profiles of the light curve arising from pulses of fireballs will not be affected by the expansion speed (that is, r is almost a constant) as long as the fireball expands relativistically. When the rest frame radiation form is taken into account, there will be a break in the curves of $r - \log\Gamma$. The location of the break depends mainly on the adopted value of the rest frame peak frequency $\nu_{0,\mathrm{p}}$. One would reach almost the same result when a jet is considered. In addition, we utilize a sample of 48 individual GRB pulses to check the relationship between the ratio r and the expansion speed Γ. We find no significant correlation between them, and this is consistent with the theoretical analysis.

Keywords: gamma-ray bursts, gamma-rays, relativity
PACC: 6180E, 4240D

1. Introduction

Gamma-ray bursts (GRBs) have been observed and studied for more than three decades.[1] There have been many attempts to quantify pulse shapes of GRBs, where statistical and empirical approaches were employed,[2−11] and different physical processes, which refer to different assumptions, were considered.[12−22] However, the great diversity of temporal profiles is still an unsolved puzzle. There is, however, a growing consensus that many burst time profiles appear to be composed of a series of discrete and often overlapping pulses with a fast rise and an exponential decay (FRED).[2,23] It is suspected that different pulses may represent emission from distinct subevents within the gamma-ray burst source. Therefore, it is necessary to investigate the time structure of the light curve arising from individual pulses.

Due to the observed very high energy photons and short timescales, GRBs are believed to arise from a relativistic expanding fireball [24−26] or be beamed from a relativistic source.[27,28] However, regardless of GRBs arising from a spherical fireball or a jetted source, the relativistic bulk motion of the ejecta would play a role in the observation of the time structure of pulses of the sources. In the previous paper[22] we have discussed the light curve of pulses of GRBs affected by the Doppler effect of fireballs and suggested that the character of FRED is independent of the Lorentz factor as long as the factor is large enough to represent a relativistic motion, and it is independent of the structure of the local pulses. In this paper, we examine in detail how the expansion speed affects the observed time profiles of fireball sources. Our analytic model is presented in Section 2; analysis on the effect on the characteristics of the light curve arising from different forms of local pulses as well as an application to a

*Project partly supported by the Special Funds for Major State Basic Research Projects (973 Program) and the National Natural Science Foundation of China (Grant No 10273019).
†E-mail: fwzhang@hotmail.com

GRB sample are made in Section 3; and conclusions are presented in Section 4.

2. Analytic model

In this section, we present necessary formula to be used to analyse the time profiles arising from various local pulses, assuming that the Doppler effect due to the expansion speed of fireballs is in force.

Consider a relativistic fireball expanding with a constant Lorentz factor and assume that its radiation is independent of direction. According to Ref.[22], the expected count rates of fireballs is

$$C(\tau)=\frac{2\pi R_{\rm c}^3}{hcD^2\Gamma^3(1-\beta)^2}\frac{\int_{\tilde{\tau}_{\theta,\min}}^{\tilde{\tau}_{\theta,\max}}\tilde{I}(\tau_\theta)(1+\beta\tau_\theta)^2(1-\tau+\tau_\theta){\rm d}\tau_\theta\int_{\nu_1}^{\nu_2}\frac{g_{0,\nu}(\nu_{0,\theta})}{\nu}{\rm d}\nu}{(1+k\tau)^2}, \tag{1}$$

where τ is a relative observed time (its definition is presented in Ref.[22]; hereafter, referred to observation time), D is the distance between the fireball centre to the observer, θ is the angle of the concerned differential surface ${\rm d}s_\theta$ of the fireball to the line of sight, τ_θ is the relative emission time (in the observer frame; hereafter, referred to the emission time) of photons emitted from ${\rm d}s_\theta$, $\nu_{0,\theta}$ is the rest frame emission frequency corresponding to the observation frequency ν (they are related by the Doppler effect), $\tilde{I}(\tau_\theta)$ represents the development of the intensity magnitude in the observer local frame, $g_{0,\nu}(\nu_{0,\theta})$ describes the rest frame radiation mechanism, Γ is the Lorentz factor, h is the Planck constant, c is the speed of light, $R_{\rm c}$ is a constant, $\beta\equiv\sqrt{\Gamma^2-1}/\Gamma$, $k\equiv\beta/(1-\beta)$.

Let the emission time τ_θ be confined within

$$\tau_{\theta,\min}\le\tau_\theta\le\tau_{\theta,\max}. \tag{2}$$

According to Ref.[22], for the whole fireball surface, which corresponds to

$$\theta_{\min}=0 \qquad \text{and} \qquad \theta_{\max}=\pi/2, \tag{3}$$

the observation time τ would be confined within

$$(1-\beta)\tau_{\theta,\min}\le\tau\le 1+\tau_{\theta,\max}, \tag{4}$$

while the integral limits of τ_θ in equation (1), $\tilde{\tau}_{\theta,\min}$ and $\tilde{\tau}_{\theta,\max}$, would be determined by

$$\tilde{\tau}_{\theta,\min}=\max\{\tau-1,\tau_{\theta,\min}\} \tag{5}$$

and

$$\tilde{\tau}_{\theta,\max}=\min\left\{\frac{\tau}{1-\beta},\tau_{\theta,\max}\right\} \tag{6}$$

respectively. In addition, $\nu_{0,\theta}$ and ν are related by

$$\nu_{0,\theta}=\frac{(1+k\tau)(1-\beta)\Gamma}{1+\beta\tau_\theta}\nu. \tag{7}$$

Recently, many observations show that GRB fireball is not spherical but conical or jetted.[27,28] The radiation from a relativistic source is beamed with a typical beaming angle $1/\Gamma$.[26] Assuming that the jet is a cone (a uniform jet) facing the observer and is confined by

$$\theta_{\min}=0 \qquad \text{and} \qquad \theta_{\max}=\frac{1}{\Gamma}, \tag{8}$$

then one gets

$$\tilde{\tau}_{\theta,\min}=\max\left\{\tau_{\theta,\min},\frac{\tau-1+\cos\frac{1}{\Gamma}}{1-\beta\cos\frac{1}{\Gamma}}\right\}, \tag{9}$$

$$\tilde{\tau}_{\theta,\max}=\min\left\{\tau_{\theta,\max},\frac{\tau}{1-\beta}\right\} \tag{10}$$

and

$$(1-\beta)\tau_{\theta,\min}\le\tau\le 1-\cos\frac{1}{\Gamma}+\left(1-\beta\cos\frac{1}{\Gamma}\right)\tau_{\theta,\max}. \tag{11}$$

With Eq.(1) and these formulae, the relation between the width of pulses and the Lorentz factor would be well determined as long as the form of local pulses and the rest frame radiation mechanism are provided.

3. Effect on the characteristics of the light curves arising from different forms of local pulses

In this paper we focus our attention mainly on how the temporal structure is affected by the expansion speed of fireballs, where different forms of local pulses with the same FWHM and the same peak intensity are considered.

Let the FWHM W_0 and the peak intensity I_0 be the same, respectively, for different local pulse forms

adopted below. Six local pulses considered are as follows: (a) a rectangle one

$$\tilde{I}(\tau_\theta) = \begin{cases} I_0 & (0 \le \tau_\theta \le W_0) \\ 0 & (\tau_\theta < 0 \ \text{ and } \ \tau_\theta > W_0) \end{cases}; \qquad (12)$$

(b) a linear rise and linear decay one

$$\tilde{I}(\tau_\theta) = I_0 \begin{cases} \dfrac{\tau_\theta}{W_0} & (0 \le \tau_\theta \le W_0) \\ 2 - \dfrac{\tau_\theta}{W_0} & (W_0 < \tau_\theta \le 2W_0) \end{cases}; \qquad (13)$$

(c) a linear rise and exponential decay one

$$\tilde{I}(\tau_\theta) = I_0 \begin{cases} \dfrac{\tau_\theta}{W_0} & (0 \le \tau_\theta \le W_0) \\ \exp\left(\log(0.5)\dfrac{\tau_\theta - W_0}{0.5W_0}\right) & (W_0 < \tau_\theta \le \tau_{\theta,\max}) \end{cases}; \qquad (14)$$

(d) an exponential rise and exponential decay one

$$\tilde{I}(\tau_\theta) = I_0 \begin{cases} \exp\left(-\log(0.5)\dfrac{\tau_\theta - 10W_0}{0.5W_0}\right) & (\tau_{\theta,\min} \le \tau_\theta \le 10W_0) \\ \exp\left(\log(0.5)\dfrac{\tau_\theta - 10W_0}{0.5W_0}\right) & (10W_0 < \tau_\theta \le \tau_{\theta,\max}) \end{cases}; \qquad (15)$$

(e) an exponential rise and linear decay one

$$\tilde{I}(\tau_\theta) = I_0 \begin{cases} \exp\left(-\log(0.5)\dfrac{\tau_\theta - 10W_0}{0.5W_0}\right) & (\tau_{\theta,\min} \le \tau_\theta \le 10W_0) \\ 11 - \dfrac{\tau_\theta}{W_0} & (10W_0 < \tau_\theta \le 11W_0) \end{cases}; \qquad (16)$$

(f) a Gaussian one

$$\tilde{I}(\tau_\theta) = I_0 \exp\left(\frac{1}{(0.5W_0)^2}\log(0.5)(\tau_\theta - 10W_0)^2\right) \qquad (\tau_{\theta,\min} \le \tau_\theta \le \tau_{\theta,\max}). \qquad (17)$$

In order to describe the characteristics of the light curves of the local pulses, let us consider the ratio r of the FWHM width of the rising phase of the light curve to that of the decaying phase. This quantity was employed by several authors[2,11,12] to study burst asymmetry properties in the past and interesting correlations between the pulse asymmetries and other temporal properties were found.

A well-known radiation form of GRBs is the so-called Band function,[29] which was commonly employed to fit the spectra of GRBs.[30−33] The Band function can be written as

$$g_{0,\nu,B}(\nu_{0,\theta}) = \begin{cases} \left(\dfrac{\nu_{0,\theta}}{\nu_{0,\mathrm{p}}}\right)^{1+\alpha_0} \exp\left[-(2+\alpha_0)\dfrac{\nu_{0,\theta}}{\nu_{0,\mathrm{p}}}\right] & \left(\dfrac{\nu_{0,\theta}}{\nu_{0,\mathrm{p}}} < \dfrac{\alpha_0-\beta_0}{2+\alpha_0}\right) \\ \left(\dfrac{\alpha_0-\beta_0}{2+\alpha_0}\right)^{\alpha_0-\beta_0} \exp(\beta_0-\alpha_0)\left(\dfrac{\nu_{0,\theta}}{\nu_{0,\mathrm{p}}}\right)^{1+\beta_0} & \left(\dfrac{\nu_{0,\theta}}{\nu_{0,\mathrm{p}}} \ge \dfrac{\alpha_0-\beta_0}{2+\alpha_0}\right) \end{cases}, \qquad (18)$$

where subscript "B" represents the word "Band", "p" stands for "peak", α_0 and β_0 are the lower and higher Band spectral indices, respectively. Typical values coming from statistical analysis of the lower and higher indices of the Band function are $\alpha_0 = -1$ and $\beta_0 = -2.25$, respectively.[32,33] According to Qin,[34] the shape of rest frame spectra is not significantly changed by the expansion of fireballs. We take $g_{0,\nu}(\nu_{0,\theta}) = g_{0,\nu,B}(\nu_{0,\theta})$ and adopt $\alpha_0 = -1$ and $\beta_0 = -2.25$ to study the effect of the expansion speed of fireballs on the light curves arising from different forms of local pulses. Shown in Figs.1 and 2 are the curves of $r - \log\Gamma$ corresponding to the cases of the local pulses considered above for a spherical fire-

ball, where we take $\pi R_c^3 I_0/hcD^2 = 1$, $\nu_1/\nu_{0,p} = 100$, $\nu_2/\nu_{0,p} = 300$, $\tau_{\theta,\min} = 0$ and $\tau_{\theta,\max} \to \infty$. We find from the two figures that the impact of the expansion speed on the temporal structure of the light curve arising from the local pulses is obvious. It can be seen from these figures that the trend between r and $\log \Gamma$ is almost the same for all cases concerned. In the curve of r— $\log \Gamma$, there are $r_{\max}$, $r_{\min}$, and a "break", which appears in the middle of curves for all the adopted forms of local pulses, when the expanding motion of the fireball is relativistic ($\Gamma > 5$). Listed in Table 1 are the characteristics of the curves in Figs.1 and 2. From the table one can find that the location of the break, $\Gamma_{\rm break}$, is hardly affected by the adopted form of the local pulses (the value of $\Gamma_{\rm break}$ is almost the same for all the cases concerned).

Comparing the temporal characteristics shown in Figs.1 and 2, one finds that both the form and the FWHM of local pulses play important roles (see also Ref.[22]). However, as shown in equation (1), besides these two elements, there might be two other factors possibly affecting the time profile, which are the rest frame radiation form and the expansion speed of fireballs.

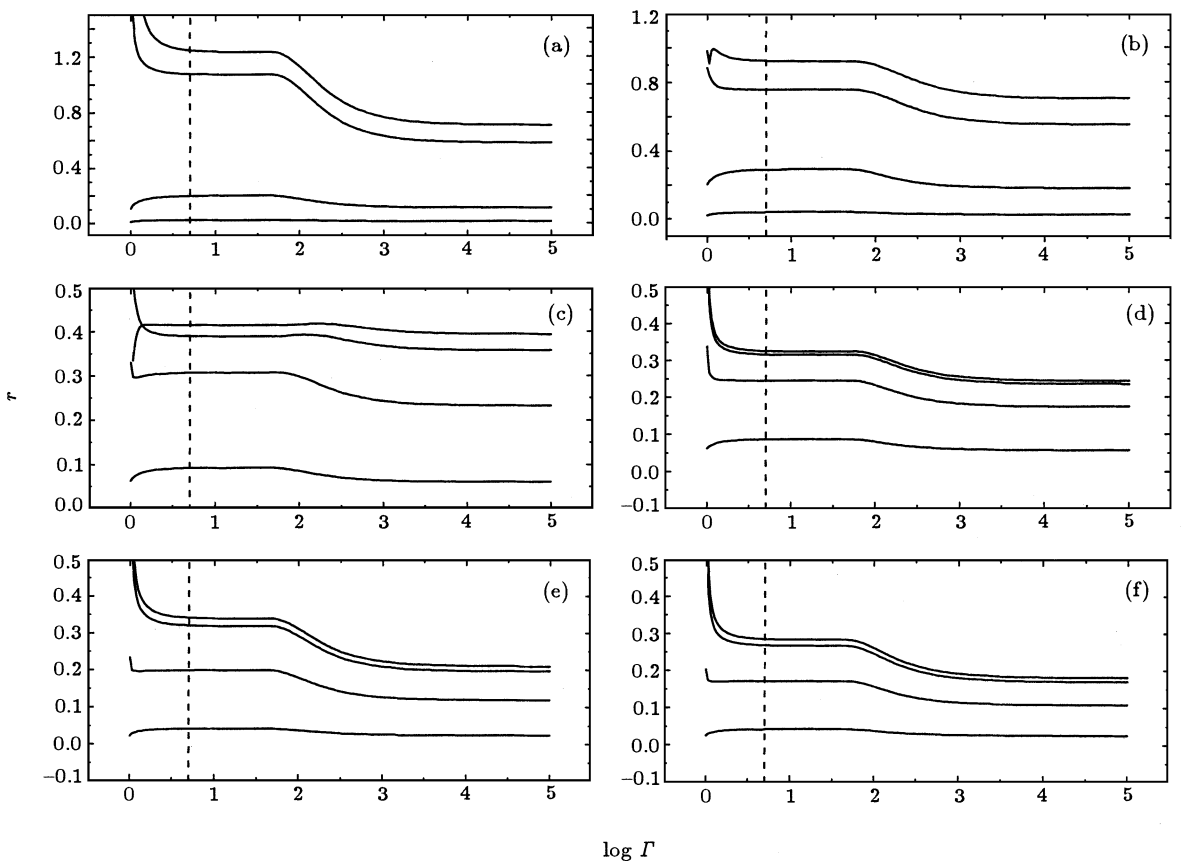


Fig.1. Plots of $r - \log \Gamma$ for the curves arising from different forms of local pulses in the spherical fireball model, where a Band function rest frame radiation form is adopted. The solid lines from the bottom to the top represent the FWHM of the local pulse $W_0 = 0.01$, 0.1, 1.0, 10.0, respectively. The local pulse forms we considered are as follows: a rectangle one (a), a linear rise and linear decay one (b), a linear rise and exponential decay one (c), an exponential rise and exponential decay one (d), an exponential rise and linear decay one (e), and a Gaussian one (f), respectively. The dashed line stands for $\Gamma = 5$.

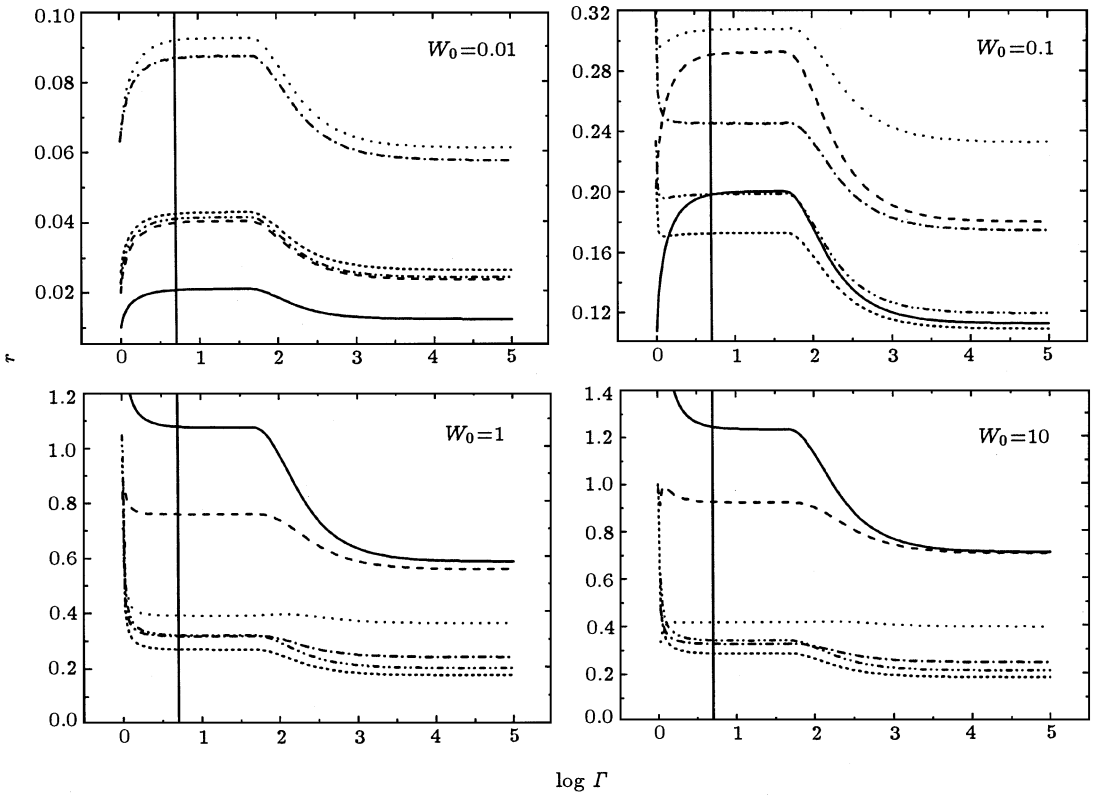


Fig.2. Plots of $r - \log \Gamma$ for the curves arising from different forms of local pulses in the spherical fireball model, where a Band function rest frame radiation form is adopted and the FWHM of the local pulses W_0 are the same, respectively. The local pulse forms we considered are as follows: a rectangle one(solid line), linear rise and a linear decay one (dash line), a linear rise and exponential decay one (dot line), an exponential rise and an exponential decay one (dash dot line), an exponential rise and linear decay one (dash dot dot line), and a Gaussian one (short dash line), respectively. The upright solid line stands for $\Gamma = 5$. The other symbols are the same as those in Fig.1.

Table 1. The characteristics of the curves shown in Figs.1 and 2.

FWHM(local)		rect	lrd	lred	erd	erld	Gau
0.01		46	46	47	45	45	46
0.10	$\Gamma_{\rm break}$	44	45	50	50	46	47
1.00		43	45	46	54	45	47
10.0		43	43	48	57	44	47
0.01		0.021	0.040	0.093	0.087	0.041	0.043
0.10	$r_{\rm max}$	0.200	0.293	0.308	0.246	0.198	0.173
1.00		1.072	0.757	0.393	0.315	0.318	0.267
10.0		1.232	0.921	0.418	0.325	0.339	0.283
0.01		0.012	0.023	0.061	0.057	0.024	0.026
0.10	$r_{\rm min}$	0.112	0.180	0.232	0.174	0.119	0.109
1.00		0.581	0.553	0.357	0.235	0.196	0.171
10.0		0.708	0.703	0.394	0.244	0.210	0.182

Note. rect=rectangle; lrd=linear rise and decay; lred = linear rise and exponential decay; erd = exponential rise and decay; erld=exponential rise and linear decay; Gau = Gaussian.

To study this issue, let us investigate if the Lorentz factor alone can lead to the characteristics observed in Figs.1 and 2 when the rest frame radiation form is ignored. Thus, we ignore the possible effect from the spectrum and assume a δ function form:

$$g_{0,\nu}(\nu_{0,\theta}) = \delta(\nu_{0,\theta} - \nu_{0,0}) \quad (\nu_{0,\min} \leq \nu_{0,\theta} \leq \nu_{0,\max}). \tag{19}$$

Replacing $g_{0,\nu}(\nu_{0,\theta})$ in equation (1) with (19), we obtain (see Ref.[22])

$$C(\tau) = \frac{2\pi R_{\rm c}^3}{\nu_0 hcD^2\Gamma^4(1-\beta)^3} \times \frac{\int_{\widetilde{\tau}_{\theta,\min}}^{\widetilde{\tau}_{\theta,\max}} \tilde{I}(\tau_\theta)(1+\beta\tau_\theta)^3(1-\tau+\tau_\theta)d\tau_\theta}{(1+k\tau)^3}, \quad (20)$$

where $\widetilde{\tau}_{\theta,\min}$ and $\widetilde{\tau}_{\theta,\max}$ are determined by (5) and (6), respectively.

Profiles of $r - \log\Gamma$ determined by (20) for the cases considered above are presented in Fig.3, where we take $\pi R_{\rm c}^3 I_0/\nu_0 hcD^2 = 1$, $\tau_{\theta,\min} = 0$ and $\tau_{\theta,\max} \to \infty$. From Fig.3 one can find that the temporal profile is not affected by the expansion speed when the rest frame radiation form is ignored, assuming that the expanding motion of fireballs is relativistic. One therefore could conclude that the characteristics shown in Figs.1 and 2 are not mainly due to the expansion speed, instead, they would depend on the rest frame radiation form.

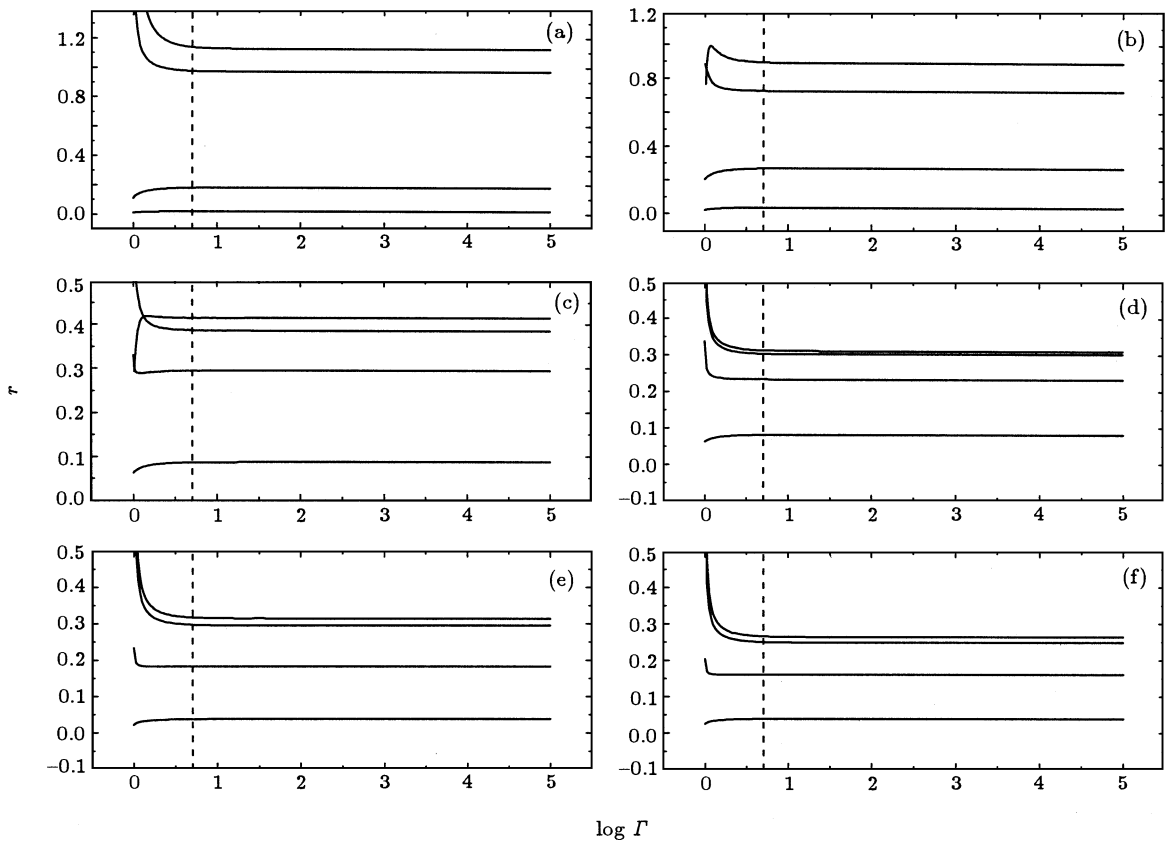


Fig.3. Plots of $r - \log\Gamma$ for the curves arising from different forms of local pulses in the spherical fireball model, where the δ rest frame spectrum is adopted. The other symbols are the same as those in Fig.1.

In addition, we take different values of $\nu_{0,\rm p}$ (the rest frame peak frequency) when adopting the same Band function to make the $r - \log\Gamma$ curve for three of the local pulses presented above, where the FWHM is taken to be the same. Shown in Fig.4 is the $r - \log\Gamma$ curves corresponding to different values of $\nu_{0,\rm p}$. It shows clearly that the rest frame radiation form plays a very important role in producing the temporal profiles of the light curve of fireballs. We also observe that the location of the break mainly depends on the adopted value of $\nu_{0,\rm p}$. The values of $\Gamma_{\rm break}$ for these cases were presented in Table 2.

Table 2. The value of $\Gamma_{\rm break}$ shown in Fig.4.

Form(local)	$\nu_{0,\rm p}$	FWHM(local)			
		0.01	0.10	1.00	10.0
rect	0.1	470	460	440	440
	1.0	46	44	43	43
	10	4.8	4.9	5.2	4.9
lrd	0.1	460	460	450	500
	1.0	46	45	45	43
	10	4.9	4.8	4.8	4.4
Gau	0.1	460	460	470	470
	1.0	46	47	47	47
	10	4.8	4.5	5.7	5.7

Note. rect = rectangle; lrd = linear rise and decay; Gau = Gaussian.

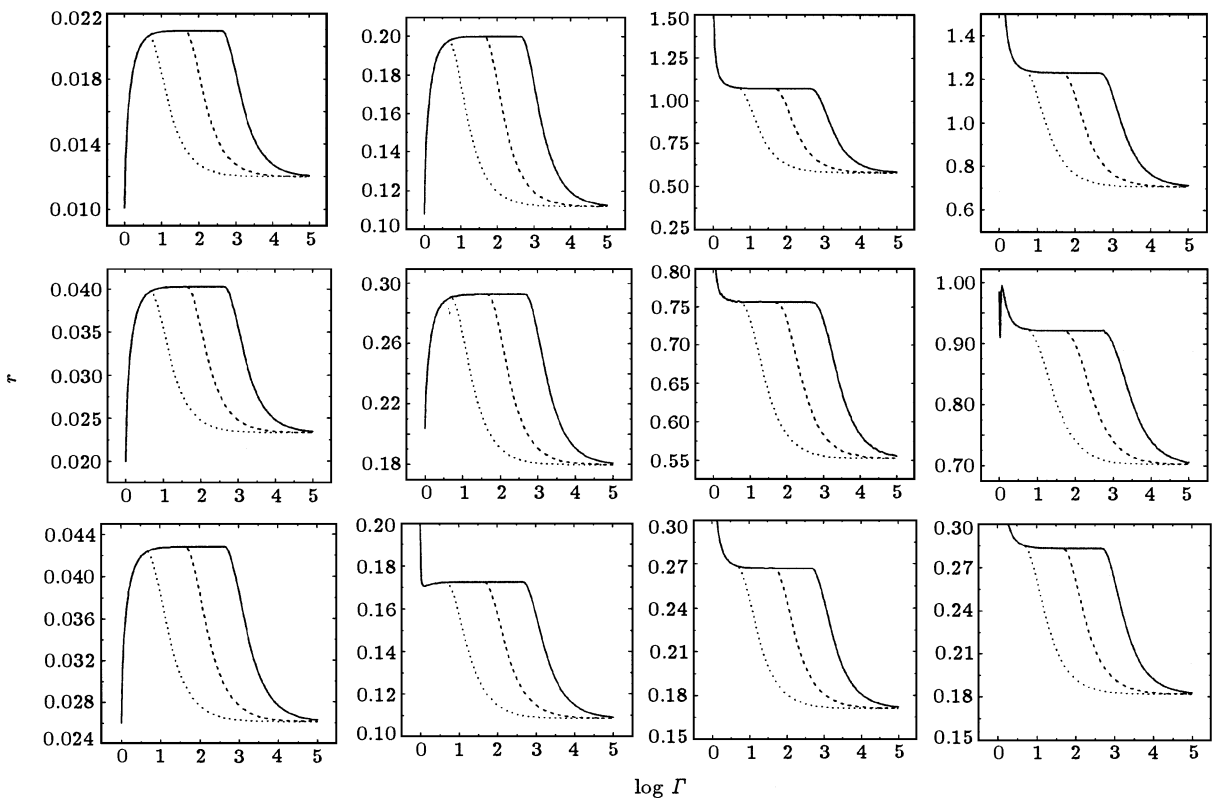


Fig.4. Plots of $r - \log\Gamma$ for the curves arising from local rectangle pulse (the first row), local linear rise and linear decay pulse (the second row), and local Gaussian pulse (the third row), respectively, where a Band function rest frame radiation form is adopted, and we take local pulse FWHM $W_0 = 0.01$ (the first column), $W_0 = 0.1$ (the second column), $W_0 = 1$ (the third column) and $W_0 = 10$ (the fourth column). The solid line stands for $\nu_{0,\rm p} = 0.1$, the dashed line represents $\nu_{0,\rm p} = 1$, the dotted line represents $\nu_{0,\rm p} = 10$.

Let us turn to study the relationship between the Lorentz factor and the observed time profiles of the local pulse for a jet for which condition (8) is applied. We consider the same case and take the same parameters as those performed above in the spherical fireball model. Shown in Figs.5 and 6 are the curves of $r - \log\Gamma$ corresponding to the Band function radiation form and the δ function radiation form for the jetted model, respectively. As can be seen from the two figures, the results are almost the same as those obtained from the spherical fireball. This can be deduced from previous studies.[12,22] Due to the Doppler effect of the relativistic sources, neglecting the area of $\theta > 1/\Gamma$ would lead a light curve with a cutoff tail, or a turn over, in its decay phase, but it does not affect the width of pulses. It shows that the expansion speed hardly affects the observed time characteristics of pulses, regardless of the radiation being emitted from a spherical fireball or a jet, as long as the expanding motion of ejecta is relativistic. It is very dif-

ficult to identify whether GRBs arise from a spherical fireball or a jet source from this relationship.

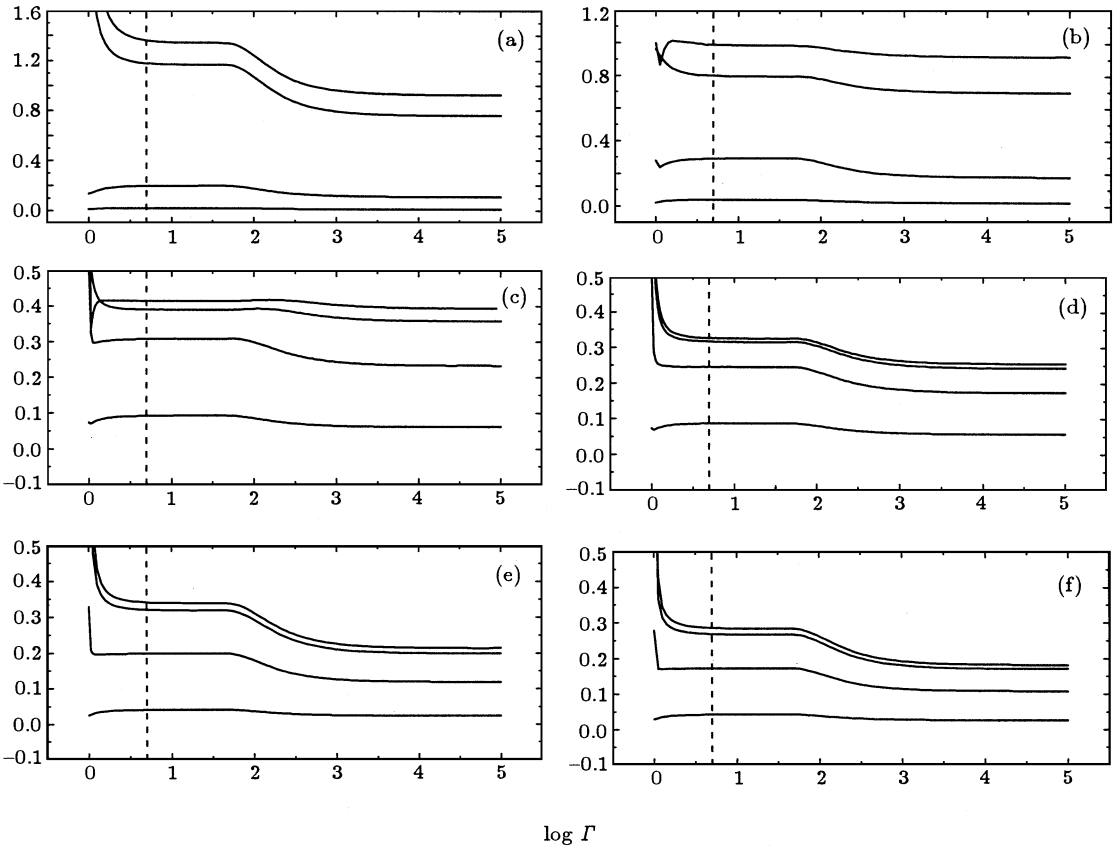


Fig.5. Plots of $r - \log \Gamma$ for the curves arising from different forms of local pulses in the jetted source model, where a Band function rest frame radiation form is adopted. The other symbols are the same as those in Fig.1.

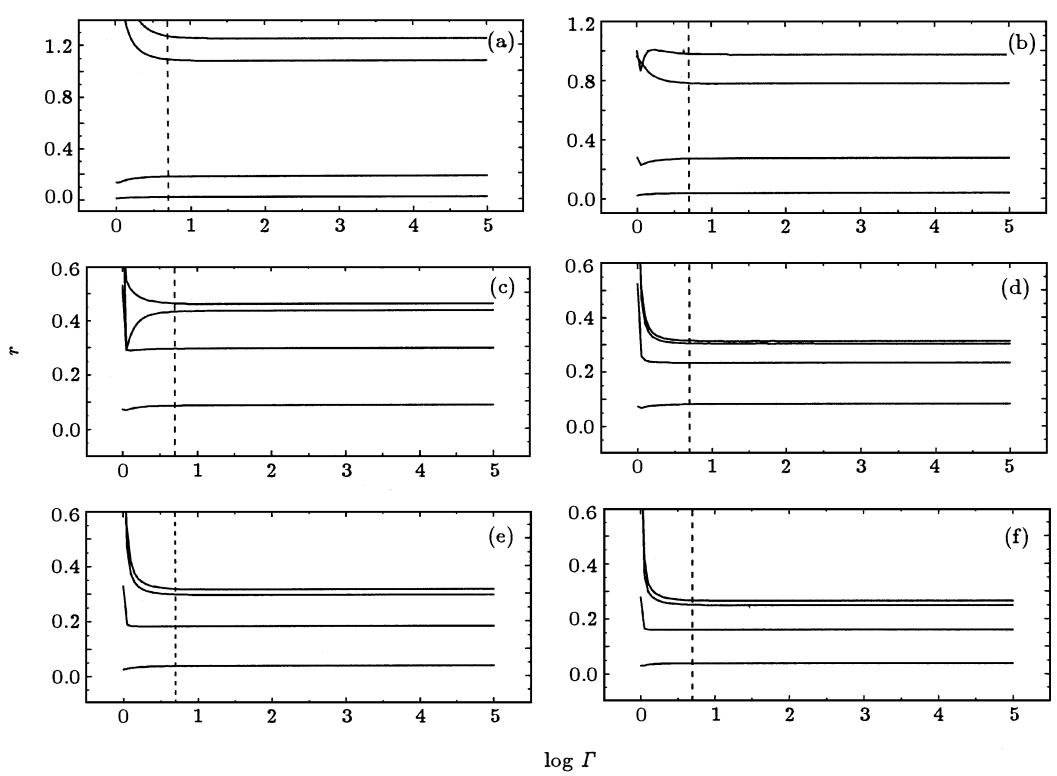


Fig.6. Plots of $r - \log \Gamma$ for the curves arising from different forms of local pulses in the jetted source model, where the δ rest frame spectrum is adopted. The other symbols are the same as those in Fig.1.

To check this relationship obtained from the above theoretical analysis, we employ a sample of 48 individual GRB pulses provided by Kocevski *et al*,[11] where the value of the νf_ν peak energy $E_{\rm p}$ of this GRB sample is taken from Mallozzi *et al.*[35] The data are listed in Table 3. We find from Qin and Zhang[34,36] that there is a linear relationship between the peak frequency $\nu_{\rm p}$ (or the peak energy $E_{\rm p}$) and Γ for the four radiation forms considered in the paper. The relationship is shown in Fig.7. The distribution of $E_{\rm p}$ (or $\nu_{\rm p}$) was once proposed[37] to scale as the bulk Lorentz factor Γ. We present here the plots of $r - \log E_{\rm p}$ for the sample adopted above (see Fig.8), which obviously show the correlation between the local pulse observed time profiles r and their peak energy $E_{\rm p}$. Assuming that the effect arising from the differences of the rest frame spectra is insignificant, the scales of $\log E_{\rm p}$ and $\log \Gamma$ would differ by a constant, and thus the plot of $r - \log E_{\rm p}$ could represent to some extent the plot of $r - \log \Gamma$. From this figure we find no significant relationship between r and $E_{\rm p}$ (the correlation coefficient is $R = 0.161$). This result is consistent with our theoretical analysis. In addition, for the sake of comparison, we also plot two curves of $r - \log \Gamma$ shown in Fig.1(b) corresponding to the local linear rise and linear decay pulse with FWHM $W_0 = 0.1$ and $W_0 = 1$ in this panel. It is plain that GRBs arising from local linear rise and linear decay pulse, whose FWHM is in 0.1 to 1, can well explain the observed result.

Table 3. The $E_{\rm p}$ and r of 48 GRBs shown in Fig.8.

Burst trigger number	$E_{\rm p}$/keV[a]	r[b]	Burst trigger number	$E_{\rm p}$/keV[a]	r[b]
563	181.7	0.31078	2919	566.6	0.46086
907	135.9	0.33844	3003	613.7	0.52856
914	116.0	0.51359	3143	240.7	0.52222
973	295.6	0.53794	3155	306.0	0.58158
999	505.9	0.56749	3256	99.39	0.33743
1157	261.4	0.41198	3257	174.2	0.29066
1406	184.5	0.44283	3259	306.2	0.55396
1467	220.4	0.55700	3290	121.3	0.46583
1733	724.2	0.48340	3415	171.1	0.42835
1883	234.6	0.52478	3648	125.7	0.45096
1956	131.3	0.56211	3765	202.4	0.45635
1989	109.7	0.52646	3870	186.4	0.37058
2083	207.5	0.45694	3875	53.94	0.38717
2102	146.2	0.57594	3886	167.0	0.49474
2138	164.3	0.65392	3892	300.0	0.51245
2193	268.1	0.43166	3954	358.7	0.53038
2387	171.0	0.52090	4157	96.03	0.53832
2484	171.9	0.55336	4350	102.0	0.47297
2519	121.7	0.38093	4368	95.61	0.54698
2530	99.78	0.46953	5478	207.4	0.46720
2662	177.8	0.34061	5495	209.1	0.32517
2665	70.93	0.42030	5517	178.3	0.61541
2700	232.0	0.44871	5523	128.7	0.59531
2880	136.9	0.46695	5541	144.8	0.55660

[a]From Mallozzi *et al*[35]

[b]From Kocevski *et al*[11]

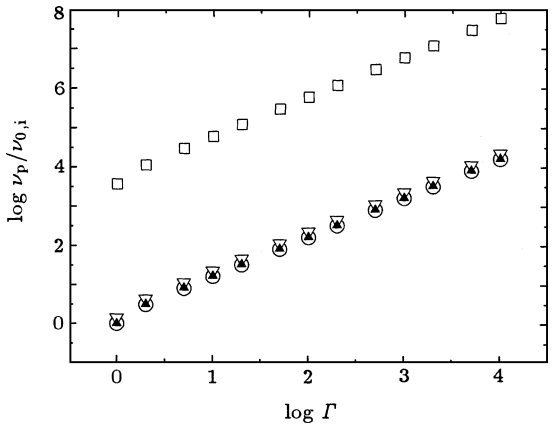


Fig.7. Plots of $\log\nu_p - \log\Gamma$ for the bremsstrahlung (open circle), Comptonized (open triangle), synchrotron (open square), and the GRB model (filled triangle) radiation, where $\log(\nu_{\rm p}/\nu_{0,\rm i})$ represents $\log(\nu_{\rm p}/\nu_{0,\rm B})$, $\log(\nu_{\rm p}/\nu_{0,\rm C})$, $\log(\nu_{\rm p}/\nu_{0,\rm S})$ and $\log(\nu_{\rm p}/\nu_{0,\rm P})$. The data are taken from Tables 1–4 in the paper of Qin and Zhang.[36].

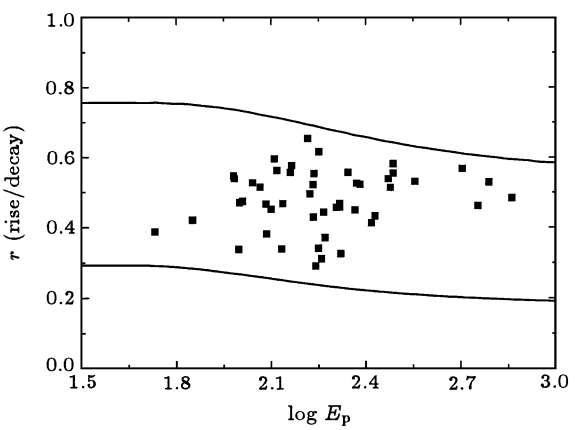


Fig.8. Plots of $r - \log E_{\rm p}$ for the sample of 48 individual GRB pulses, showing no significant correlation between the peak energy $E_{\rm p}$ (or the expansion speed Γ) and the local pulse observed time profiles r. The correlation coefficient is $R = 0.161$. Two solid lines represent the curves of $r - \log\Gamma$ corresponding to local linear rise and linear decay pulse with FWHM $W_0 = 0.1$ and $W_0 = 1$ in Fig.1(b).

4. Conclusions

In this paper, temporal profiles of gamma-ray bursts arising from different forms of local pulses are studied in the relativistic fireball framework. How the form and FWHM of local pulses plays a role and how the expansion speed of fireballs affects the time profile associated with these corresponding local pulses are investigated.

To study the temporal profile of GRB pulses, we employ the ratio of the FWHM widths of the rising phase of the light curve to that of the decaying phase, r, which represents a characteristics of light curves. In investigating the effect of the expansion speed on the light curve arising from different forms and different FWHM widths of local pulses, we find that the profile of light curves is not affected by the expansion speed as long as the expanding motion of the fireball is relativistic ($\Gamma > 5$), when the effect of spectrum is ignored. However, when taking into account the rest frame radiation form, the expansion speed will play a role in producing the profile of light curves associated with the corresponding local pulses. Due to the effect of the rest frame spectrum, there will be a break in the curve of $r - \log\Gamma$. The location of the break is hardly affected by the form of local pulses, but depends obviously on the adopted value of the rest frame peak frequency $\nu_{0,\rm p}$. In addition, we investigate the relationship between the expansion speed Γ and the observed time profiles r for a jet, and find almost the same results as those obtained in the spherical fireball model. In order to check our analytical results, we utilize a sample of 48 individual GRB pulses to study the relationship between Γ and r. We find that the observed result is consistent with our theoretical analysis. The data fall well within the curves arising from FWHM $W_0 = 0.1$ and FWHM $W_0 = 1$ of local linear rise and linear decay pulses.

Acknowledgment

We thank Dr Paciesas for kindly sending us the necessary $E_{\rm p}$ data.

References

[1] Klebesadel R W, Strong I B and Olson R A 1973 *Astrophys. J.* **182** L85
[2] Norris J P, Nemiroff R J, Bonnell J T *et al* 1996 *Astrophys. J.* **459** 393
[3] Beloborodov A M 1998 *Astrophys. J.* **508** L25
[4] Fenimore E E 1999 *Astrophys. J.* **518** 375
[5] Chang H Y and Yi I 2000 *Astrophys. J.* **542** L17
[6] Lee A, Bloom E D and Petrosian V 2000 *Astrophys. J. Suppl. Ser.* **131** 1
[7] Lee A, Bloom E D and Petrosian V 2000 *Astrophys. J. Suppl. Ser.* **131** 21
[8] Ryde F and Svensson R 2000 *Astrophys. J.* **529** L13
[9] Ryde F and Svensson R 2002 *Astrophys. J.* **566** 210
[10] Ryde F and Petrosian V 2002 *Astrophys. J.* **578** 290
[11] Kocevski D, Ryde F and Liang E 2003 *Astrophys. J.* **596** 389

[12] Fenimore E E, Madras C D and Nayakshin S 1996 *Astrophys. J.* **473** 998
[13] in't Zand J J M and Fenimore E E 1996 *Astrophys. J.* **464** 622
[14] Kobayashi S, Piran T and Sari R 1997 *Astrophys. J.* **490** 92
[15] Daigne F and Mochkovitch R 1998 *Mon. Not. Roy. Astron. Soc.* **296** 275
[16] Daigne F and Mochkovitch R 2003 *Mon. Not. Roy. Astron. Soc.* **342** 587
[17] Fenimore E E, Cooper C, Ramirez-Ruiz E *et al* 1999 *Astrophys. J.* **512** 683
[18] Panaitescu A 1999 *Astrophys. J.* **522** L105
[19] Ramirez-Ruiz E and Fenimore E E 2000 *Astrophys. J.* **539** 712
[20] Spada M, Panaitescu A and Mészáros P 2000 *Astrophys. J.* **537** 824
[21] Nakar E and Piran T 2002 *Astrophys. J.* **572** L139
[22] Qin Y P, Zhang Z B, Zhang F W and Cui X H 2004 *Astrophys. J.* **617** 439
[23] Fishman G J, Meegan C A, Wilson R B *et al* 1994 *Astrophys. J. Suppl. Ser.* **92** 229
[24] Goodman J 1986 *Astrophys. J.* **308** L47
[25] Paczynski B 1986 *Astrophys. J.* **308** L43
[26] Piran T 1999 *Phys. Rep.* **314** 575
[27] Rhoads J E 1997 *Astrophys. J.* **487** L1
[28] Sari R, Piran T and Halpern J P 1999 *Astrophys. J.* **519** L17
[29] Band D, Matteson J, Ford L *et al* 1993 *Astrophys. J.* **413** 281
[30] Schaefer B E, Teegaeden B J, Fantasia S F *et al* 1994 *Astrophys. J. Suppl. Ser.* **92** 285
[31] Ford L A, Band D L, Mattesou J L *et al* 1995 *Astrophys. J.* **439** 307
[32] Preece R D, Pendleton G N, Briggs M S *et al* 1998 *Astrophys. J.* **496** 849
[33] Preece R D, Briggs M S, Mallozzi R S *et al* 2000 *Astrophys. J. Suppl. Ser.* **126** 19
[34] Qin Y P 2002 *Astron. Astrophys.* **396** 705
[35] Mallozzi R S, Paciesas W S, Pendleton G N *et al* 1995 *Astrophys. J.* **454** 597
[36] Qin Y P and Zhang F W 2004 *Astron. Astrophys.* **421** 9
[37] Brainerd J J, Preece R D, Briggs M S *et al* 1998 *Astrophys. J.* **501** 325